

Doublet-singlet model and unitarity

G. Cynolter*, J. Kovács† and E. Lendvai‡

*MTA-ELTE Research Group in Theoretical Physics, Eötvös University, Budapest, 1117
Pázmány Péter sétány 1/A, Hungary*

Abstract

We study the renormalizable singlet-doublet fermionic extension of the Standard Model. In this model, the new vector-like fermions couple to the gauge bosons and to the Higgs via new Yukawa couplings, that allow for nontrivial mixing in the new sector, providing a stable, neutral dark matter candidate. Approximate analytic formulae are given for the mass spectrum around the blind spots, where the dark matter candidate coupling to h or Z vanishes. We calculate the two particle scattering amplitudes in the model, impose the perturbative unitarity constraints and establish bounds on the Yukawa couplings.

arXiv:1509.05323v2 [hep-ph] 18 Dec 2015

*cyn@general.elte.hu

†kovacsjucus@caesar.elte.hu

‡lendvai@general.elte.hu

1 Introduction

There is a renewed interest in vector-like fermions [1], as these are less constrained than chiral fermions in electroweak precision tests of the Standard Model (SM) [2, 3] and free of anomalies. Vector-like fermions appear naturally in various beyond the Standard Model scenarios, such as specific string theories, bulk fermions in universal extra dimensional models [4], little Higgs theories [5, 6], supersymmetric models as superpartners of standard bosons e.g. higgsinos [7], various composite Higgs models [8, 9] and simplified models of dark matter [10, 11, 12]. Vector-like fermions help gauge coupling unification, but the lower unification scale is in conflict with proton decay constraints [10]. A recent survey of phenomenological implications of vector-like extensions [1] presents constraints from electroweak precision observables, direct collider searches, Higgs production and decays.

The couplings to the standard light (and heavier) fermions are severely constrained. To avoid flavour problems (for flavour issues see [13]) and to ensure there is no mixing between SM and the new vector-like fermions a \mathbb{Z}_2 matter parity is introduced. The new fermions are odd, while the standard particles are even under this symmetry. The lightest new particle is stable and if it is electrically neutral then it provides a dark matter candidate. The singlet-doublet dark matter model is an effective theory or simplified version of the neutralino MSSM dark matter sector. The mixing in the dark sector allows for a wide range of Higgs and gauge boson couplings that is able to avoid direct detection in dark matter experiments and colliders and give the measured relic density, while still remaining a relatively simple model. The model contains four new parameters, two dimensionful mass parameters and two Yukawa couplings, originally completely unconstrained. A recent analysis in [14] has found combined bounds on the vector masses and the overall value of the Yukawa coupling.

The spectrum generally is a solution of a third order equation and the analytical treatment is difficult. Another problem is that the four-dimensional parameter space can be only visualized if at least two parameters (generally the Yukawas) are fixed. In [14] the phenomenologically allowed regions of the parameter space have been found in the neighborhood of the blind spots, where the coupling of the dark matter candidate to h or Z vanishes. In these special points one eigenvalue can be found and the third order equation simplifies to a second order one. With this observation we have found analytic solution for the masses close to the blind spots. We have further shown that the relevant coupling constants are small and can avoid observation by direct detection experiments.

The parameters of the model can be constrained on theoretical grounds. Perturbative unitarity is a useful tool to set limits on effective theories. Starting from weak charged current interaction, it leads to the well-known gauge bosons and the Higgs with usual couplings of the SM. It provided an upper bound on its validity without the Higgs boson and a theoretical upper bound on the Higgs mass [15]. For chiral fermions, there is also an upper bound on the scale of fermion mass generation in the few TeV region [16]. In this paper we calculate the two-particle scattering amplitudes involving the new fermions, aiming to constrain the free parameters of the model. As the new part of the Lagrangian is renormalizable, the potentially dangerous amplitudes growing with energy cancel each other. The elastic scattering of neutral fermions of the doublet and the singlet gives a meaningful amplitude, constraining the value of new Yukawa couplings. The new vector-like fermions only partially receive their masses from the Higgs, therefore the new bound, $\frac{|y_{1,2}|v}{\sqrt{2}} \leq 1.23 \text{ TeV}$ cannot be directly translated to the mass of the dark matter candidate or to the mass parameters of the model.

In section 2 we review the singlet-doublet vector-like fermion extension of the Standard Model, then comment on the current dark matter bounds. In section 4 we give analytic formulae around the experimentally favored regions. In section 5 we calculate the new two-particle scattering processes that can contribute to bound the model parameters from perturbative unitarity. The paper is closed with conclusion.

2 The model

We extend the Standard Model with a pair of $SU(2)_W$ doublet Weyl-fermions, $\psi_1 = \begin{pmatrix} \psi_1^0 \\ \psi_1^- \end{pmatrix}$ and $\psi_2 = \begin{pmatrix} \psi_2^+ \\ \psi_2^0 \end{pmatrix}$, that acquire a Dirac mass term together and a singlet, χ^0 with a Majorana mass term. All three are color-singlet to avoid the strong collider bounds, their quantum numbers are listed in Table 1. We also assume a matter parity-like \mathbb{Z}_2 symmetry that forbids the new fermions to couple directly to the SM ones. The new particles then only couple to the Higgs and gauge bosons in pairs, so the Lagrangian can be break up into two parts, $\mathcal{L} = \mathcal{L}_{SM} + \mathcal{L}_{DS}$.

	T_3	Q	$Y = Q - T_3$
ψ_1^0	$\frac{1}{2}$	0	$-\frac{1}{2}$
ψ_1^-	$-\frac{1}{2}$	-1	$-\frac{1}{2}$
ψ_2^+	$\frac{1}{2}$	+1	$\frac{1}{2}$
ψ_2^0	$-\frac{1}{2}$	0	$\frac{1}{2}$
χ^0	0	0	0
h	$-\frac{1}{2}$	0	$\frac{1}{2}$

Table 1: The weak quantum numbers of the new fermions and the Higgs.

The Lagrangian for the new fermions contains their kinetic and mass terms and Yukawa couplings.

$$\mathcal{L}_{DS} = \frac{i}{2} \left(\chi^{0\dagger} \bar{\sigma}^\mu \partial_\mu \chi^0 + \psi_1^\dagger \bar{\sigma}^\mu D_\mu \psi_1 + \psi_2^\dagger \bar{\sigma}^\mu D_\mu \psi_2 \right) - \left(m_d \psi_1 \psi_2 + \frac{1}{2} m_s \chi^0 \chi^0 + y_1 \psi_1 H \chi^0 + y_2 \psi_2 \tilde{H} \chi^0 + h.c. \right) \quad (1)$$

There are two new dimensionful mass parameters and two dimensionless Yukawa couplings, (m_d, m_s, y_1, y_2) . The three phases of $\psi_{1,2}$ and χ^0 can be fixed by setting three parameters (e.g. m_d, m_s, y_1) to be real and positive. We will consider the case where y_2 is real¹ and emphasize that the sign of y_2/y_1 is physical.

A nice and widely used parametrization of the Yukawas is

$$y_1 = y \cos \theta, \quad y_2 = y \sin \theta. \quad (2)$$

The decoupled MSSM bino-higgsino system with one light Higgs corresponds to $\beta = \theta$, and y is related to the $U(1)$ gauge coupling.

The charged fermions, ψ_1^- and ψ_2^+ merge into a Dirac fermion, $\Psi^- = \begin{pmatrix} \psi_1^- \\ \psi_2^{+\dagger} \end{pmatrix}$ with mass m_d . Without the Yukawa couplings, the neutral part of the doublets also form a Dirac fermion with mass m_d , $\Psi^0 = \begin{pmatrix} \psi_1^0 \\ \psi_2^{0\dagger} \end{pmatrix}$. As the Higgs gets a vacuum expectation value with non-vanishing Yukawa couplings, there is a mixing in the new neutral sector.

$$\mathcal{L}_{DS} \supset -\frac{1}{2} \begin{pmatrix} \chi^0 & \psi_1^0 & \psi_2^0 \end{pmatrix} M_n \begin{pmatrix} \chi^0 \\ \psi_1^0 \\ \psi_2^0 \end{pmatrix} + h.c., \quad (3)$$

with the mass matrix M_n ,

$$M_n = \begin{pmatrix} m_s & \frac{y_1 v}{\sqrt{2}} & \frac{y_2 v}{\sqrt{2}} \\ \frac{y_1 v}{\sqrt{2}} & 0 & m_d \\ \frac{y_2 v}{\sqrt{2}} & m_d & 0 \end{pmatrix}. \quad (4)$$

The corresponding characteristic equation follows,

$$(m_s - \lambda) (\lambda^2 - m_d^2) + m_d y_1 y_2 v^2 + \lambda \frac{(y_1^2 + y_2^2) v^2}{2} = 0. \quad (5)$$

The cubic equation can be solved analytically using the Cardano formula or numerically. There is a negative eigenvalue that can be flipped to be positive, multiplying the corresponding eigenvector by i or equivalently performing the Takagi diagonalization on the system and get only the positive masses. Generally the spectrum contains three neutral Majorana fermions, the mass eigenstates χ_1, χ_2, χ_3 . The lightest will be denoted by χ with mass m_χ , that will be stable due to the \mathbb{Z}_2 symmetry. It is an ideal dark matter candidate if lighter than the charged fermion $m_\chi < m_d$, made from the following composition of the weak eigenstates,

$$\chi = U_{11} \chi^0 + U_{12} \psi_1^0 + U_{13} \psi_2^0, \quad |U_{11}|^2 + |U_{12}|^2 + |U_{13}|^2 = 1. \quad (6)$$

U_{11}^2 characterizes the amount of the singlet in χ . When $m_d > m_s$, χ is more singlet- or bino-like with $U_{11}^2 > 0.5$, while when $m_d < m_s$, χ is more doublet- or higgsino-like with $U_{11}^2 < 0.5$.

¹It can have a CP-violating phase, which is discussed in [10].

3 Dark matter constraints

The singlet-doublet model for various values of the parameters can provide a wino- or a higgsino-like dark matter candidate. The parameters of the model and the dark matter candidate were recently explored in [17, 18, 19, 20].

Several experiments constrain dark matter candidates. Planck observations [21] on the relic density abundance $\Omega_{dm} h^2 \simeq 0.12$. Indirect searches obtained by Fermi-LAT [22] and IceCube [23], and direct dark matter searches by PICO [24], LUX [25] and XENON100 [26]. In the low mass region, collider bounds are becoming important, too, as the charged fermion mass is already excluded for $m_d < 100$ GeV by chargino searches at LEP [27] and the LHC can study the production and annihilation of the dark matter particle [28] or the invisible Higgs and Z decays.

The most stringent bounds are coming from the direct detection experiments in the low mass region. Here the relevant couplings of the dark matter are the ones to the Higgs and Z . It is important to note that the $c_{h\chi\chi}$ coupling is related to the characteristic equation. After differentiating (5) with respect to the Higgs VEV, it can be solved for $\frac{\partial m_\chi}{\partial v} = c_{h\chi\chi}$.

$$c_{h\chi\chi} = -\frac{(2y_1 y_2 m_d + (y_1^2 + y_2^2) m_\chi) v}{m_d^2 + (y_1^2 + y_2^2) \frac{v^2}{2} + 2m_s m_\chi - 3m_\chi^2}, \quad (7)$$

$$c_{Z\chi\chi} = -\frac{m_z v (y_1^2 - y_2^2) (m_\chi^2 - m_d^2)}{2(m_\chi^2 - m_d^2)^2 + v^2 (4y_1 y_2 m_\chi m_d + (y_1^2 + y_2^2) (m_\chi^2 + m_d^2))}, \quad (8)$$

where m_χ is the eigenvalue, which can be negative as well.

The spin-independent "blind spots" [29] are defined, where $c_{h\chi\chi}$ coupling vanishes, similarly the spin-dependent blind spots, where $c_{Z\chi\chi}$ coupling vanishes. These points evade the related direct detection bounds. To keep the couplings small and avoid overabundance in the relic density, the annihilation cross section needs enhancement. This can be achieved, if there is a pole in the s-channel processes, e.g. $m_\chi \approx \frac{m_h}{2}$ or $\frac{m_z}{2}$ [17]. A recent work [14] collected all these bounds on the singlet-doublet model, including dark matter searches and colliders. It carries out a full numerical study to cover the parameter space, that includes a higher mass region, where $m_\chi > 100$ GeV and a light mass region, both illustrated with three representative Yukawa couplings y .

In the large mass region, indirect detection constrains the underabundant region in the parameter space. For the smaller Yukawas $y \leq 0.01$ that is the only bound and $m_\chi \gtrsim 280$ GeV with $U_{11}^2 \gtrsim 0.5$ remains available for any $\tan \theta$. For the more 'MSSM-like' $y = 0.2$, it allows $m_\chi \gtrsim 220$ GeV with $U_{11}^2 \gtrsim 0.65$. Here the direct detection experiments are relevant for thermal χ with $\Omega_\chi h^2 \approx 0.12$, in the region where $m_s \approx m_d$ LUX excludes up to $m_\chi \sim 1$ TeV mass. In the third region with larger Yukawas $y = 1$, they obtained $m_\chi \gtrsim 275$ GeV, unless it is purely singlet ($U_{11}^2 \gtrsim 0.8$).

In the light mass region χ is singlet-like as we mentioned, the allowed regions are around the blind spots with $m_\chi \approx \frac{m_h}{2}$ or $\frac{m_z}{2}$, but these are further constrained by the invisible Higgs decay. Parametrically, for the smaller Yukawa coupling $y = 0.1$, χ is excluded in the $80 \text{ GeV} \lesssim m_\chi \lesssim 220 \text{ GeV}$ range with $U_{11}^2 \lesssim 0.65$, and there is no further bounds on the $y = 1$ region.

The experiments bound the parameter space, but four parameters are challenging to interpret. In the next section we explore analytically the regions around the blind spots.

4 Regions of small couplings

The bounds from direct detection experiments can be fulfilled with small dark matter couplings to the Higgs and Z bosons (7, 8). The LUX [25] and XENON100 [26] experiments set bounds on the spin independent (and dependent) cross section giving for a dark matter heavier than the nucleon [29] $c_{h\chi\chi} \leq 0.01 - 0.1$ and similarly $c_{Z\chi\chi} \leq 0.01 - 0.1$ depending on the dark matter mass. In this section we study analytically the region around the blind spots, the experimentally favored regions of the parameter space [14].

The blind spots are the following,

$$c_{Z\chi\chi} = 0, \text{ if } |y_1| = |y_2| \text{ or } |m_\chi| = m_d \quad (9)$$

and

$$c_{h\chi\chi} = 0, \text{ if } m_\chi + \sin(2\theta)m_d = 0, \quad (10)$$

where $\sin(2\theta) = \frac{2y_1 y_2}{y_1^2 + y_2^2}$. The conditions in (9) are not independent. If $\lambda = \pm m_d$ is an eigenvalue of the characteristic equation (5) it follows that $y_1 = \mp y_2$ or $\tan \theta = \mp 1$. Therefore it is enough to study the cases in the neighborhood of $y_1 = \pm y_2$ and (10). Similarly if $c_{h\chi\chi}$ vanishes, it follows from (5) that the corresponding eigenvalue m_χ is $\pm m_d$ or m_s . In both cases the cubic equation remarkably simplifies by finding one root (m_d or m_s) and the rest is a quadratic equation. The expansion is performed around these special points.

Small $c_{Z\chi\chi}$, $y_1 \simeq -y_2$, $\tan \theta \simeq -1$

The mass eigenvalues are

$$m_1 = m_d(1 - x_-), \quad \text{where} \quad x_- = \frac{(y_1 + y_2)^2 v^2}{4m_d(m_s - m_d) + y^2 v^2}, \quad (11)$$

$$m_{2,3} = \frac{m_s - m_d}{2} \pm \frac{1}{2} \sqrt{(m_s + m_d)^2 + 2y^2 v^2} + \frac{m_d}{2} x_- \left(1 \mp \frac{m_s - 3m_d}{\sqrt{(m_s + m_d)^2 + 2y^2 v^2}} \right), \quad (12)$$

where $y^2 = y_1^2 + y_2^2$. The first two terms in (12) are the exact solution of the second order remnant of the characteristic equation for $m_\chi = m_d$ in the $c_{Z\chi\chi} = 0$ blind spot. The correction is proportional to x_- .² The spectrum in the blind spot $y_1 = -y_2$ is shown in Fig. 1.

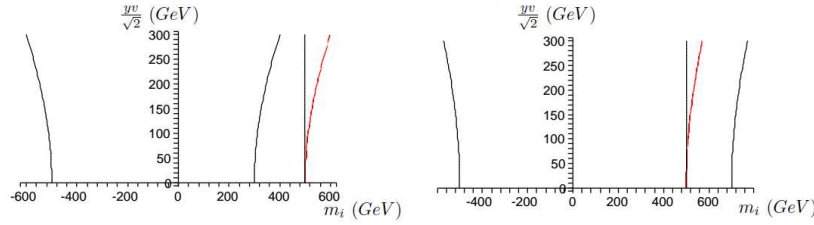


Figure 1: Mass eigenvalues for $y_1 = -y_2$ vs. increasing overall Yukawa terms $\frac{yv}{\sqrt{2}}$ for $m_s = 300 \text{ GeV} < m_d = 500 \text{ GeV}$ on the left and $m_s = 800 \text{ GeV} > m_d = 500 \text{ GeV}$ on the right. The negative eigenvalue (m_3) has been flipped to positive value and both are shown.

For $m_s < m_d$, the dark matter candidate is the one with mass m_2 , until $y < \frac{2}{v} \sqrt{m_d(m_d - m_s)}$, then m_2 becomes larger than m_1 . Its couplings are

$$c_{h\chi\chi} = \frac{8y^2 v}{m_s + m_d}, \quad c_{Z\chi\chi} = \frac{(y_1^2 - y_2^2)m_Z v}{2(m_s^2 - m_d^2)}. \quad (13)$$

We see that the Z coupling scales according to the blind spot condition ($y_1 + y_2$), but small Higgs coupling requires small overall Yukawa, y and relatively large $m_s + m_d$ compared to the Higgs VEV.

For $m_d < m_s$ or $y > \frac{2}{v} \sqrt{m_d(m_d - m_s)}$, the dark matter candidate is mostly doublet like and its mass is m_1 . The couplings are

$$c_{h\chi\chi} = \frac{(y_1 + y_2)^2 v m_d}{2m_d(m_d - m_s) - y^2 v^2}, \quad c_{Z\chi\chi} = \frac{(y_1^2 - y_2^2)m_Z v}{4m_d(m_s - m_d) + 2y^2 v^2}. \quad (14)$$

Both couplings go to zero with $(y_1 + y_2)^2$ and $(y_1 + y_2)$ multiplied with small mass ratios for non-degenerate mass parameters $|m_s - m_d| > v$. This is the most favored region to avoid direct detection even in the presence of sizable Yukawa interactions if they are tuned ($y_1 + y_2 \simeq 0$).

There is a smooth limit for $m_s = m_d$

$$c_{h\chi\chi} = -\frac{(y_1 + y_2)^2 m_d}{y^2 v}, \quad c_{Z\chi\chi} = \frac{(y_1^2 - y_2^2)m_Z}{2y^2 v}. \quad (15)$$

The Higgs coupling goes to zero with $(y_1 + y_2)^2$, while the Z coupling scales with $y_1 + y_2$ as before.

²The real expansion parameter for small $c_{Z\chi\chi}$ in equation (5) is $\frac{m_d(y_1 \mp y_2)^2 v^2}{(2m_s^2 + 6m_d^2 + 3y^2 v^2)^{\frac{3}{2}}}$, which has positive definite denominator.

Small $c_{Z\chi\chi}$, $y_1 \simeq y_2$, $\tan \theta \simeq 1$

The mass eigenvalues are

$$m_1 = -m_d(1 + x_+), \quad \text{where} \quad x_+ = \frac{(y_1 - y_2)^2 v^2}{4m_d(m_s + m_d) + y^2 v^2}, \quad (16)$$

$$m_{2,3} = \frac{m_s + m_d}{2} \pm \frac{1}{2} \sqrt{(m_s - m_d)^2 + 2y^2 v^2} + \frac{m_d}{2} x_+ \left(1 \mp \frac{m_s + 3m_d}{\sqrt{(m_s - m_d)^2 + 2y^2 v^2}} \right). \quad (17)$$

The spectrum is similar to the first case and it is shown in Fig. 2.

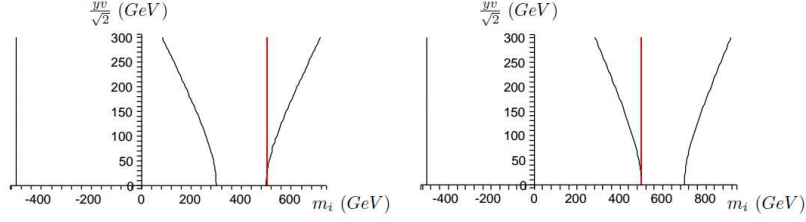


Figure 2: Mass eigenvalues for $y_1 = y_2$ vs. increasing overall Yukawa terms $\frac{yv}{\sqrt{2}}$ for $m_s = 300 \text{ GeV} < m_d = 500 \text{ GeV}$ on the left and $m_s = 800 \text{ GeV} > m_d = 500 \text{ GeV}$ on the right. The negative eigenvalue (m_1) has been flipped to positive value and both are shown.

The lightest fermion with mass m_3 is the dark matter candidate. Its mass starts from m_s or m_d and decreases as the Yukawa couplings are increased.

The Z coupling goes to zero with $y_1 - y_2$ in agreement with the blind spot condition, assuming $y^2 v^2 \ll |m_s^2 - m_d^2|$ for the sake of simplicity

$$c_{Z\chi\chi} = (y_1^2 - y_2^2) \frac{m_Z v}{2(m_d^2 - m_s^2)} \text{ for } m_s < m_d, \quad (18)$$

and

$$c_{Z\chi\chi} = (y_1^2 - y_2^2) \frac{m_Z v}{2m_d(m_s - m_d)} \text{ for } m_s > m_d. \quad (19)$$

The leading behavior of the Higgs coupling constant for $m_\chi = m_3$ is for $m_s \neq m_d$

$$c_{h\chi\chi} = \frac{y^2 v}{|m_d - m_s|}. \quad (20)$$

The Higgs coupling is small only if the Yukawa mass correction $\left(\frac{yv}{\sqrt{2}}\right)$ is smaller than the doublet-singlet mass splitting.

For $m_s = m_d$ the couplings are

$$c_{h\chi\chi} = -y_1, \text{ and } c_{Z\chi\chi} = \frac{(y_1^2 - y_2^2) m_Z}{(2m_d - y_1 v)}. \quad (21)$$

The Z coupling can be small for tuned Yukawas and if the new vectors are heavier than the Z , but the small Higgs coupling needs small y_1 .

Small $c_{h\chi\chi}$, $\sin 2\theta \simeq -\frac{m_\chi}{m_d}$

As we mentioned the Higgs blind spot is at $m_\chi = \pm m_d$ or $m_\chi = m_s$. If $|m_\chi| \simeq m_d$ then $|\tan \theta| \simeq 1$ and it is discussed in the previous two points. The non-trivial new case is when $m_\chi \simeq m_s < m_d$. The mass eigenvalues are

$$m_1 = m_s(1 - z), \quad \text{where} \quad z = \frac{2\frac{m_d}{m_s} y_1 y_2 v^2 + y^2 v^2}{2m_d^2 - 2m_s^2 + y^2 v^2}, \quad (22)$$

$$m_{2,3} = \pm \sqrt{m_d^2 + \frac{y^2 v^2}{2}} - z \left(\frac{m_s^2}{\sqrt{m_d^2 + \frac{y^2 v^2}{2}}} \mp m_s \right). \quad (23)$$

The square root is the exact solution of the second order remnant of the characteristic equation in the $c_{h\chi\chi} = 0$ blind spot for $m_\chi = m_s$ and the correction is proportional to z .³ The spectrum is shown in Fig. 3.

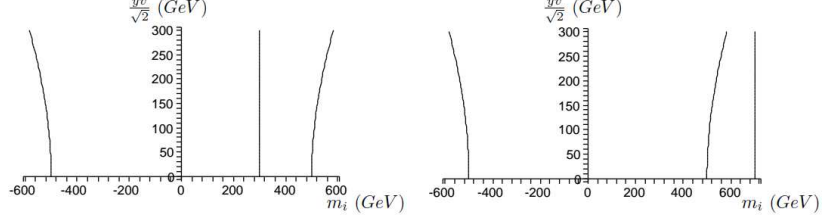


Figure 3: Mass eigenvalues for $c_{h\chi\chi} = 0$ vs. increasing overall Yukawa terms $\frac{yv}{\sqrt{2}}$ for $m_s = 300 \text{ GeV} < m_d = 500 \text{ GeV}$ on the left and $m_s = 800 \text{ GeV} > m_d = 500 \text{ GeV}$ on the right. The negative eigenvalue m_3 has been flipped to positive value and it coincides with m_2 .

The coupling constants for the $m_\chi = m_1$ dark matter candidate are

$$c_{h\chi\chi} = 4z \frac{m_s}{v}, \quad c_{Z\chi\chi} = \frac{(y_2^2 - y_1^2)m_Z v}{4m_d(m_d - m_s) + 2y^2 v^2}. \quad (24)$$

Small Z boson-dark matter coupling requires additional tuning. The $\frac{y_2}{y_1}$ ratio is fixed by $\frac{m_s}{m_d}$, therefore for non-degenerate masses $m_d - m_s \geq yv$, $c_{Z\chi\chi}$ scales with $y^2 \frac{vm_Z}{m_d \sqrt{m_s^2 - m_d^2}}$. In case of $m_s = m_d$ we get back the first case and both coupling constants (15) are small.

We have seen the exclusions and limits in the parameter space, but there are no bounds on the individual parameters. In the following section, we aim to set bounds on the four parameters one by one by exploring the consequences of perturbative unitarity.

5 Perturbative unitarity

Perturbative unitarity is an essential tool in exploring effective field theories. Amplitudes growing with energy indicate the breakdown of the effective theory and the validity range of the model can be estimated or new particles and interactions can be added to cancel the terms with bad high energy behavior. In the SM, the complete gauge structure of the W , Z and Higgs interactions can be recovered and there are cancellations due to gauge symmetry. Unitarity still constrains the parameters of the SM, the Higgs self coupling, which can be translated to the Higgs mass [15]. Later, the method was applied to massive chiral fermions without a Higgs boson. It was shown in [16] that the scattering amplitude of a fermion-antifermion pair to longitudinally polarized gauge bosons must be unitarized below 3.5 TeV in the case of the top quark, constraining the scale of fermion mass generation, e.g. giving an upper bound on the validity of the model.

Here, we investigate tree-level elastic two-particle scattering processes. Considering the $J = 0$ partial-wave amplitude and we require perturbative unitarity for a process with scattering amplitude \mathcal{M} and scattering angle θ .

$$a_0 = \frac{1}{32\pi} \int_{-1}^1 d(\cos \theta) |\mathcal{M}|, \quad |\text{Re} a_0| \leq \frac{1}{2} \quad (25)$$

There are four relevant processes in the model. Charged fermion pair annihilation to W 's, charged and neutral fermion annihilation to W and Higgs, two charged fermions scattering through Z and γ and finally, neutral fermions scattering through Higgs exchange. The amplitudes are included for each helicity channel of the fermions for energies much higher than any masses, $\sqrt{s} \gg m_W$.

³The expansion parameter for small $c_{h\chi\chi}$ in (5) is $\frac{(m_s \frac{y^2}{2} + m_d y_1 y_2) v^2}{(2m_s^2 + 6m_d^2 + 3y^2 v^2)^{\frac{3}{2}}}$.

$$\Psi^-(s_1)\Psi^+(s_2) \rightarrow W^-W^+$$

The Feynman graphs for the process are shown in Fig. 4. In the t-channel we have three graphs with the three neutral mass eigenstates, $\chi_{1,2,3}$. Since we sum up all possible internal particles, if we do a unitary transformation on $\chi_{1,2,3}$ and sum up all the new states, we get the same result. That means, we can calculate with the electroweak eigenstates, $\Psi^0 = \begin{pmatrix} \psi_1^0 \\ \psi_2^0 \end{pmatrix}$ and χ^0 , where χ^0 's couplings are zero. The amplitude is then

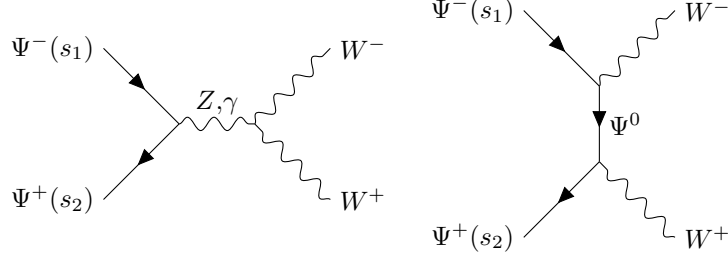


Figure 4: Feynman graphs for $\Psi^-\Psi^+ \rightarrow W^-W^+$ scattering.

$$\mathcal{M}_{s_1 s_2}(\Psi^-\Psi^+ \rightarrow W^-W^+) = \begin{pmatrix} \frac{g^2(1-\tan^2\theta_w)}{4} \sin\theta + \mathcal{O}\left(\frac{m_W^2}{s}\right) & \mathcal{O}\left(\frac{m_W}{\sqrt{s}}\right) \\ \mathcal{O}\left(\frac{m_W}{\sqrt{s}}\right) & -\frac{g^2(1-\tan^2\theta_w)}{4} \sin\theta + \mathcal{O}\left(\frac{m_W^2}{s}\right) \end{pmatrix} \quad (26)$$

In the amplitude matrix, the incoming fermion helicity channels are the following,

$$(s_1 \ s_2) : \begin{pmatrix} -- & -+ \\ +- & ++ \end{pmatrix}. \quad (27)$$

As in the case of chiral fermions [16], the s-channel amplitudes grow with s , that cancel with the Z and γ exchange graphs. The t-channel grows with \sqrt{s} , but here it is canceled by the s-channel graphs and there is no need for the otherwise absent Higgs exchange.

$$\Psi^-(s_1)\chi_i(s_2) \rightarrow W^-h$$

The charged and a neutral fermion can annihilate into a W and Higgs, illustrated in Fig. 5. In the t-channel internal lines, we can use again the weak eigenstate Ψ^0 . Naively using the weak eigenstates as the initial states, we find that the $\Psi^-\chi^0 \rightarrow W^-h$ scattering process grows with \sqrt{s} , while there is no problem with the other process $\Psi^-\Psi^0 \rightarrow W^-h$ (the helicities of the fermions are as in (27)).

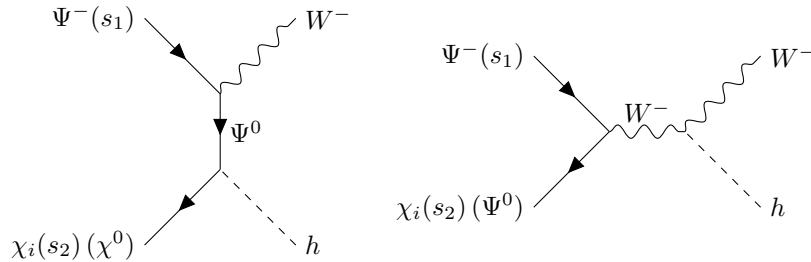


Figure 5: Feynman graphs for the $\Psi^-\chi_i \rightarrow W^-h$ scattering.

$$\mathcal{M}_{s_1 s_2}(\Psi^-\chi^0 \rightarrow W^-h) = \begin{pmatrix} 0 & \frac{gy_2\sqrt{s}}{2m_W} + \mathcal{O}\left(\frac{m_W}{\sqrt{s}}\right) \\ -\frac{gy_1\sqrt{s}}{2m_W} + \mathcal{O}\left(\frac{m_W}{\sqrt{s}}\right) & 0 \end{pmatrix} \quad (28)$$

$$\mathcal{M}_{s_1 s_2}(\Psi^-\Psi^0 \rightarrow W^-h) = \begin{pmatrix} -\frac{g^2 \sin\theta_w}{2\sqrt{2}} & 0 \\ 0 & \frac{g^2 \sin\theta_w}{2\sqrt{2}} \end{pmatrix} + \mathcal{O}\left(\frac{m_W}{\sqrt{s}}\right) \quad (29)$$

But taking the mass eigenstates $\chi_{1,2,3}$, that mixes Ψ^0 and χ^0 , makes the s-channel graph grows with \sqrt{s} compensating the t-channel. The whole process becomes unitary and leaving the highest order to be proportional to $g^2 \sin \theta_w$ and a combination of the mixing matrix elements.

$$\Psi^-(s_1)\Psi^+(s_2) \rightarrow \Psi^-(s_3)\Psi^+(s_4)$$

The charged fermions can scatter through s- and t-channel Z and γ exchange illustrated with Feynman graphs in Fig. 6.

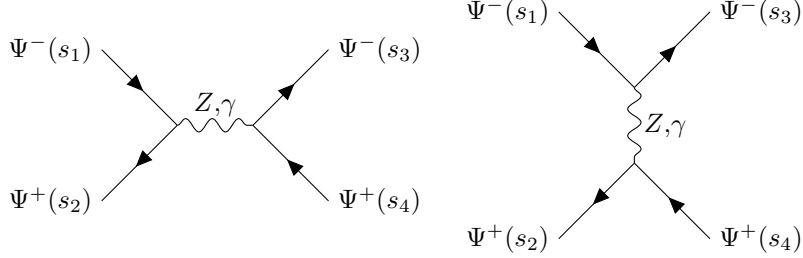


Figure 6: Feynman graphs for $\Psi^-\Psi^+ \rightarrow \Psi^-\Psi^+$ scattering.

$$\mathcal{M}_{s_1 s_2 s_3 s_4}(\Psi^-\Psi^+ \rightarrow \Psi^-\Psi^+) = \begin{pmatrix} \frac{g^2 \sin^2 \frac{\theta}{2}}{2 \cos^2 \theta_w} & 0 & 0 & \frac{g^2 \cos^2 \frac{\theta}{2}}{2 \cos^2 \theta_w} \\ 0 & 0 & \frac{-g^2}{2 \cos^2 \theta_w} & 0 \\ 0 & \frac{-g^2}{2 \cos^2 \theta_w} & 0 & 0 \\ \frac{g^2 \cos^2 \frac{\theta}{2}}{2 \cos^2 \theta_w} & 0 & 0 & \frac{g^2 \sin^2 \frac{\theta}{2}}{2 \cos^2 \theta_w} \end{pmatrix} + \mathcal{O}\left(\frac{m_W^2}{s}\right) \quad (30)$$

For the two-to-two fermion scattering amplitudes the sixteen fermion helicity channels are in the following order,

$$(s_1 \quad s_2 \quad s_3 \quad s_4) : \begin{pmatrix} - & - & - & - & - & - & + & - & - & - & - & - & + & - & - & - \\ - & - & + & - & - & - & + & + & - & - & - & - & + & + & - & - \\ + & - & - & - & + & - & - & + & - & - & + & + & - & - & + & - \\ + & - & + & - & + & - & + & + & - & + & + & - & + & + & + & - \end{pmatrix}. \quad (31)$$

In the first two processes, the growing terms in the amplitude cancel each other because of the gauge symmetry. The remaining term, just as in the previous two processes, is proportional to the gauge coupling and satisfy the unitarity constraint (25).

$$\Psi^0(s_1)\chi^0(s_2) \rightarrow \Psi^0(s_3)\chi^0(s_4)$$

The neutral fermion scattering can be still interesting, since this process includes Higgs boson exchange and the corresponding unconstrained Yukawa couplings. The related Feynman graph is shown in Fig. 7. This process is basically the $\chi_i \chi_j \rightarrow \chi_k \chi_l$ mass eigenstate scattering. But since there is only one type of graph contributing, which is proportional to some combination of the Yukawa couplings, $y_{1,2}$, we can mix these processes to get the $\Psi^0 \chi^0 \rightarrow \Psi^0 \chi^0$ weak eigenstate scattering with the following amplitude.

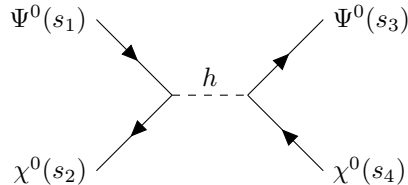


Figure 7: Feynman graphs for $\Psi^0 \chi^0 \rightarrow \Psi^0 \chi^0$ scattering.

$$i\mathcal{M}(\Psi_{s_1}^0(p_1)\chi_{s_2}^0(p_2) \rightarrow h(q_s) \rightarrow \Psi_{s_3}^0(p_3)\chi_{s_4}^0(p_4)) = \left(\frac{i}{2\sqrt{2}}\right)^2 (\bar{v}_{s_2}(p_2)(y_+ + y_- \gamma_5)u_{s_1}(p_1)) \frac{i}{s - m_h^2} (\bar{u}_{s_3}(p_3)(y_+ + y_- \gamma_5)v_{s_4}(p_4)) \quad (32)$$

Where the shorthand notations of the couplings are $y_{\pm} = y_1 \pm y_2$.

$$\mathcal{M}_{s_1 s_2 s_3 s_4}(\Psi^0 \chi^0 \rightarrow \Psi^0 \chi^0) = \begin{pmatrix} 0 & 0 & 0 & 0 \\ 0 & \frac{y_+^2}{2} + \mathcal{O}\left(\frac{m_h^2}{s}\right) & -\frac{y_1 y_2}{2} + \mathcal{O}\left(\frac{m_h^2}{s}\right) & 0 \\ 0 & -\frac{y_1 y_2}{2} + \mathcal{O}\left(\frac{m_h^2}{s}\right) & \frac{y_+^2}{2} + \mathcal{O}\left(\frac{m_h^2}{s}\right) & 0 \\ 0 & 0 & 0 & 0 \end{pmatrix} \quad (33)$$

The fermion helicity channels are in the same order as in the charged fermion scattering in (31).

Now using a_0 partial-wave unitarity (25) for the non-zero elements in the amplitude matrix, we get a bound on the Yukawa couplings.

$$|y_{1,2}| \leq 4\sqrt{\pi} \approx 7.1 \quad |y_1 y_2| \leq 16\pi \approx 50.3 \quad (34)$$

The Yukawa contributions to the fermion masses are bounded by

$$\frac{|y_{1,2}|v}{\sqrt{2}} \leq 2\sqrt{2}\pi v \approx 1.23 \text{ TeV}, \quad (35)$$

where $v = 246 \text{ TeV}$ is the Higgs VEV.

We see that perturbative unitarity sets meaningful bounds on the so far unconstrained new Yukawa couplings. The other processes are proportional to the gauge coupling and the bounds are automatically satisfied.

6 Conclusion

We have studied the vector-like fermionic singlet-doublet extension of the Standard Model. This is a minimal, gauge invariant and renormalizable model, motivated by dark matter. It has four free parameters, two masses and two Yukawa couplings. A \mathbb{Z}_2 matter parity is introduced, the lightest neutral mass eigenstate can be the dark matter candidate. As a result of the mixing between the doublet and the singlet there are tree-level couplings of the dark matter to the Z and Higgs bosons and the couplings can vary in a wide range. This model is a consistent simplified version of UV complete supersymmetric theories, such as the bino-higgsino sector of the MSSM or the singlino-higgsino sector of the naturalness motivated NMSSM-like models. The main difference from the MSSM bino-higgsino system is that the Yukawa couplings are free parameters here and not related to the hypercharge coupling and $\tan \beta$. The effective or simplified model is ideal to test the parameters with experiments.

To have a better view and analytic control of the parameters, we have calculated the mass eigenvalues and the relevant Z , h couplings in the neighborhood of the blind spots. We identified the best region allowed by direct detection experiments, where $m_d < m_s$ and the not necessary small Yukawas are tuned to nearly cancel each other $y_1 + y_2 \simeq 0$. There are other blind spot regions, where the Yukawas (y) must be small. Direct and indirect dark matter searches constrain the combined parameter space, but not the individual parameters of the model, still leaving room for a "WIMP miracle". To set bounds on separate parameters, we have calculated two particle scattering amplitudes in the model. Applied the bounds of perturbative unitarity and found that no amplitude has bad high energy behavior as expected from renormalizability. There are no constraints on the Dirac- and Majorana-mass. The new Yukawa couplings appear in s-channel Higgs exchange graphs and are bounded $|y_{1,2}| < 7.1$. The LHC phenomenology of the model is studied e.g. in [1, 14]. The medium and the low mass region can be tested at the $\sqrt{s} = 13 \text{ TeV}$ LHC in the next few years [14].

References

- [1] S. A. R. Ellis, R. M. Godbole, S. Gopalakrishna and J. D. Wells, JHEP **1409** (2014) 130 [arXiv:1404.4398 [hep-ph]].
- [2] G. Cynolter and E. Lendvai, Eur. Phys. J. C **58** (2008) 463 [arXiv:0804.4080 [hep-ph]].
- [3] A. Joglekar, P. Schwaller and C. E. M. Wagner, JHEP **1212** (2012) 064 [arXiv:1207.4235 [hep-ph]].

- [4] T. Appelquist, H. C. Cheng and B. A. Dobrescu, Phys. Rev. D **64** (2001) 035002 [hep-ph/0012100].
- [5] N. Arkani-Hamed, A. G. Cohen, E. Katz and A. E. Nelson, JHEP **0207** (2002) 034 [hep-ph/0206021].
- [6] N. Arkani-Hamed, A. G. Cohen, E. Katz, A. E. Nelson, T. Gregoire and J. G. Wacker, JHEP **0208** (2002) 021 [hep-ph/0206020].
- [7] N. Arkani-Hamed and S. Dimopoulos, JHEP **0506** (2005) 073 [hep-th/0405159].
- [8] R. Contino, L. Da Rold and A. Pomarol, Phys. Rev. D **75** (2007) 055014 [hep-ph/0612048].
- [9] G. Cynolter, E. Lendvai and G. Pocsik, Eur. Phys. J. C **46** (2006) 545 [hep-ph/0509230].
- [10] R. Mahbubani and L. Senatore, Phys. Rev. D **73** (2006) 043510 [hep-ph/0510064].
- [11] R. Enberg, P. J. Fox, L. J. Hall, A. Y. Papaioannou and M. Papucci, JHEP **0711** (2007) 014 [arXiv:0706.0918 [hep-ph]].
- [12] F. D'Eramo, Phys. Rev. D **76** (2007) 083522 [arXiv:0705.4493 [hep-ph]].
- [13] K. Ishiwata, Z. Ligeti and M. B. Wise, arXiv:1506.03484 [hep-ph].
- [14] L. Calibbi, A. Mariotti and P. Tziveloglou, arXiv:1505.03867 [hep-ph].
- [15] B. W. Lee, C. Quigg and H. B. Thacker, Phys. Rev. D **16** (1977) 1519.
- [16] T. Appelquist and M. S. Chanowitz, Phys. Rev. Lett. **59** (1987) 2405 [Phys. Rev. Lett. **60** (1988) 1589].
- [17] T. Cohen, J. Kearney, A. Pierce and D. Tucker-Smith, Phys. Rev. D **85** (2012) 075003 [arXiv:1109.2604 [hep-ph]].
- [18] C. Cheung, M. Papucci and K. M. Zurek, JHEP **1207** (2012) 105 [arXiv:1203.5106 [hep-ph]].
- [19] C. Cheung and D. Sanford, JCAP **1402** (2014) 011 [arXiv:1311.5896 [hep-ph]].
- [20] J. Halverson, N. Orlofsky and A. Pierce, Phys. Rev. D **90** (2014) 1, 015002 [arXiv:1403.1592 [hep-ph]].
- [21] P. A. R. Ade *et al.* [Planck Collaboration], Astron. Astrophys. **571** (2014) A16 [arXiv:1303.5076 [astro-ph.CO]].
- [22] M. Ackermann *et al.* [Fermi-LAT Collaboration], arXiv:1503.02641 [astro-ph.HE].
- [23] M. G. Aartsen *et al.* [IceCube Collaboration], Phys. Rev. Lett. **110** (2013) 13, 131302 [arXiv:1212.4097 [astro-ph.HE]].
- [24] C. Amole *et al.* [PICO Collaboration], Phys. Rev. Lett. **114** (2015) 23, 231302 [arXiv:1503.00008 [astro-ph.CO]].
- [25] D. S. Akerib *et al.* [LUX Collaboration], Phys. Rev. Lett. **112** (2014) 091303 [arXiv:1310.8214 [astro-ph.CO]].
- [26] E. Aprile *et al.* [XENON100 Collaboration], Phys. Rev. Lett. **111** (2013) 2, 021301 [arXiv:1301.6620 [astro-ph.CO]].
- [27] J. Abdallah *et al.* [DELPHI Collaboration], Eur. Phys. J. C **31** (2003) 421 [hep-ex/0311019].
- [28] R. Enberg, P. J. Fox, L. J. Hall, A. Y. Papaioannou and M. Papucci, JHEP **0711** (2007) 014 [arXiv:0706.0918 [hep-ph]].
- [29] C. Cheung, L. J. Hall, D. Pinner and J. T. Ruderman, JHEP **1305** (2013) 100 [arXiv:1211.4873 [hep-ph]].